KINEMATIC GPS: PERFORMANCE AND QUALITY CONTROL

C.C.J.M. Tiberius, P.J.G. Teunissen and P.J. de Jonge
Delft Geodetic Computing Centre (LGR)
Faculty of Geodesy
Delft University of Technology
Thijsseweg 11
2629 JA Delft, The Netherlands
e-mail: lgr@geo.tudelft.nl

BIOGRAPHY

Peter Teunissen is professor in Mathematical Geodesy and Positioning. Christian Tiberius and Paul de Jonge both graduated at the Faculty of Geodetic Engineering of the Delft University of Technology. They are currently engaged in the development of GPS data processing strategies for, respectively, kinematic surveying applications and networks.

ABSTRACT

This contribution presents and discusses practical results of kinematic GPS that can typically be achieved. The results are based on a kinematic experiment using a mobile receiver on a van and two stationary receivers. The van is driven from one of the stationary receivers to a distance of over 10 km. Highlighted are the quality of the positioning results, the system's ability to test for outliers in the code data and cycle slips in the phase data, and the numerical and statistical performance of ambiguity resolution. The results are given for different measurement scenarios, such as satellite redundancy and single versus dual frequency data.

1 INTRODUCTION

When linking the mathematical model to the data, care has to be excercized in formulating the observations equations (functional model) and the covariance matrix of the observables (stochastic model). In case of GPS, the set of observables that can be used consists of carrier phases and pseudoranges (code) on L_1 and L_2. These observables can be linked to the baseline coordinates and the carrier phase ambiguities. Apart from these unknown parameters, the observation equations may also include additional parameters, such as those needed for ionospheric and troposheric refraction, or for the (receiver and/or satellite) clock errors, or for the signal delays in the hardware or for multipath [1-4]. Whether or not all these parameters need to be included as well, depends very much on the hardware used, the circumstances of measurement and the particular application at hand.

For kinematic GPS, fast and reliable ambiguity resolution is a prerequisite [5-7]. This is feasible when the uncertainty in the atmospheric delays, in particular the ionospheric delays, can be sufficiently bounded. Short baseline applications are therefore the first applications that come in mind when thinking of kinematic GPS [8-12]. In this contribution we therefore restrict our attention to the short baseline case and analyse, on the basis of an experiment, the performance of kinematic GPS using the simplest mathematical model possible.

For the undifferenced code observables, the standard deviation was set at $\sigma_p = 0.3$ m, and for the undifferenced phase observables, it was set at $\sigma_\phi = 0.003$ m. Time-correlation was assumed absent. The differential atmospheric delays were also assumed absent, because of the relatively short baselines. The only unknown parameters in the double differenced (DD) observation equations were therefore the DD carrier phase ambiguities and the components of the three dimensional baselines. The data were processed in the single-baseline mode. For the kinematic case, the linear(ized) system of DD observation equations of epoch i reads then

$$y(i) = Aa + B(i)b(i) + e(i) \quad \text{for } i = 1, \ldots, k \qquad (1)$$

where the vector $y(i)$ consists of the observed minus computed single or dual frequency phase and code observations of epoch i, a is the time-invariant vector of unknown integer DD ambiguities, $b(i)$ is the unknown increment of the nonstationary baseline at epoch i, $e(i)$ contains the measurement noises and remaining unmodelled effects, and A and $B(i)$ are the appropriate design matrices.

The above system of observation equations was solved using the *recursive* least-squares algorithm. Since the

International Symposium on Kinematic Systems
in Geodesy, Geomatics and Navigation KIS97
Banff, Canada, June 3-6, 1997

ambiguities are time-invariant (in the absence of cycle slips) and the baselines are unconnected in time, the *time-update* has a rather simple form. Only the (float) least-squares estimate of the ambiguity vector needs to be passed on in time. The actual filter step is performed in the *measurement-update*. In this step the incoming data is adjusted together with the results provided by the time-update.

After a brief description of the experiment in Sect. 2, we consider in Sect. 3 the system's ability to test for, respectively, outliers in the code data and cycle slips in the phase data. Since the data processing is based on the recursive least-squares algorithm, it are the so-called predicted residuals that contain all the necessary information to perform the three steps of detection, identification and adaptation [13]. The minimal detectable biases are given for the case the ambiguities are still floated and for the case the ambiguities are fixed.

In Sect. 4 we consider the problem of ambiguity resolution. It consists of the integer estimation step and the validation step. The estimation step is solved using the least-squares ambiguity decorrelation adjustment. For validation we first consider the ambiguity dilution of precision to infer the system's potential strength for a successful fixing of the ambiguities. This is followed with an analysis of the actual performance of ambiguity resolution. In the last section, Sect. 5, we concentrate on the positioning performance itself and show results of baseline repeatibility.

2 THE EXPERIMENT

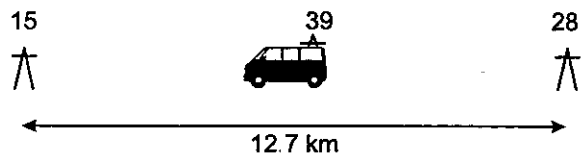

Figure 1: Two stationary receivers 15 and 28, with roving receiver 39.

In this section we will describe the experiment on which our data analysis is based. The experiment took place on December 22^{nd}, 1996, about 80 km North-East from Delft, on the Oostvaardersdijk from Almere to Lelystad, along the Markermeer. Three dual frequency geodetic receivers were used (Trimble 4000 SSI Geodetic Surveyor). Two of the receivers were placed stationary on parking-lots (points 15 and 28), about 12.7 km apart. The antenna of the third receiver was rigidly mounted on the roof of the faculty's van (point 39), see figure 1.

The data used was collected during a 40 minute session, at a one second sampling rate, when the van drove from point 15 to point 28 and back again. During the whole session, the same 7 satellites (PRN's 04, 10, 16, 19, 24, 27 and 18) were continuously tracked, all at an elevation angle larger than 15 degrees. The corresponding skyplot is shown in figure 2. We also consider configurations with less than seven satellites. They were obtained by removing, respectively, PRN's 24, 19 and 27. The circumstances during the session concerned typical weather for this season of the year: open sky, temperature a few degrees below 0 Celsius and a strong wind blowing from the North-East. The Sun Spot Number was low, about 20-30, and the (absolute) ionospheric delay was small.

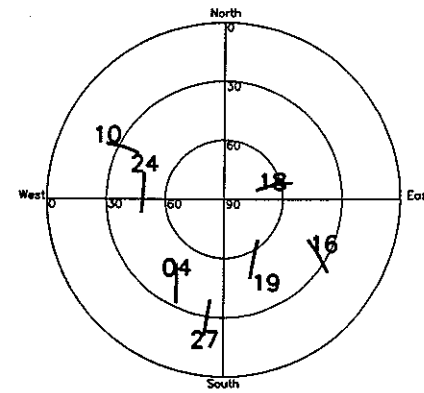

Figure 2: Skyplot (12-22-'96, 08:30 UTC, $\phi = 52°26'$N, $\lambda = 5°14'$E), with PRN's 04, 10, 16, 18, 19, 24, 27.

3 SPIKES AND SLIPS

It will be clear that the results of an adjustment rely heavily on the validity of the functional and stochastic model used. Errors in one of the two, or in both, will invalidate these results. Apart from the adjustment itself, one therefore also needs to make use of methods that allow one to check the validity of the assumptions underlying the model. These methods are based on the theory of statistical testing.

3.1 DIA PROCEDURE

One way of structuring a testing procedure for the handling of different model errors is provided by the DIA-procedure [13-15]. It consists of the following three steps:

1. *Detection*: An overall model test is performed to diagnose whether an unspecified model error ocurred.
2. *Identification*: After detection of a model error, identification of the potential source of model error is needed.

3. *Adaptation:* After identification of a model error, adaptation of the null hypothesis is needed to eliminate the presence of biases in the solution.

The DIA-procedure can be applied *locally* or *globally* In the latter case, a time window is used such that the data within the window is used for the testing. The global tests, which can also be computed recursively, have the advantage of a higher detection power than the local tests. Paired with this advantage goes the disadvantage of a possible delay in detection. In the present contribution only the local DIA-procedure was used

When using the recursive least-squares algorithm, the so-called *predicted* residuals come available at every epoch with almost no extra effort. The predicted residual vector of epoch i, $v(i)$, is defined as the difference between the vector of observables of that epoch and its prediction. It can be shown that the predicted residuals, together with their variance matrices, contain all the information necessary to perform the statistical testing

For detection purposes, first a local overall model (LOM) test is applied. The corresponding test statistic is given as

$$T(k) = \frac{v(k)^T Q_{v(k)}^{-1} v(k)}{m(k)} \qquad (2)$$

where $m(k)$ denotes the number of observations that enter at epoch k. When the data are normally distributed (which is assumed throughout this contribution), this test statistic has a central Chi-square distribution divided by its degrees of freedom $m(k)$. Note that in case of the overall model test, no specification of the type of model error is needed yet. For identification however, one needs to specify explicitly the type of model error that is likely to occur. In case of GPS there are in particular two type of model errors that are worth testing for. They are the outliers (spikes) in the code data and the slips in the phase data. For both these potential model errors, the appropriate test statistic, which has a standard normal distribution under the null hypothesis, takes the form

$$t(k) = \frac{c^T Q_{v(k)}^{-1} v(k)}{\sqrt{c^T Q_{v(k)}^{-1} c}} \qquad (3)$$

where the c-vector still needs to be specified. In case of local testing this vector equals the DD matrix operator times a canonical unit vector. For an outlier, the nonzero entry of the unit vector corresponds with the suspected single differenced code observable. For a slip, its nonzero entry corresponds with the suspected single differenced phase observable.

3.2 MINIMAL DETECTABLE BIASES

Internal reliability as represented by the Minimal Detectable Biases (MDB's), describes the size of the model errors which can just be detected with the appropriate test statistics. For the test statistic (3), the MDB is given as

$$\mathrm{MDB} = \sqrt{\frac{\lambda_0}{c^T Q_{v(k)}^{-1} c}} \qquad (4)$$

where λ_0 is the reference value of the noncentrality parameter. It depends on the chosen level of significance and on the chosen power. The level of significance was set at 0.001 and the power at 0.80.

For the current experiment, we computed both the code-MDB's and the phase-MDB's. Values which are considered representative for these MDB's are shown in figures 3, 4, 5 and 6 as function of the number of satellites tracked. The first two figures refer to the code-MDB's (ambiguity-float and ambiguity-fixed) and the last two refer to the phase-MDB's (ambiguity-float and ambiguity-fixed). All the code-MDB's and the ambiguity-fixed phase-MDB's which are shown, are based on the use of a single epoch of data.

Figure 3 shows the code-MDB's for the single-frequency case and for the dual-frequency case. The MDB's get clearly larger as the number of satellites decreases. In case of four satellites (no satellite redundancy) the MDB even goes to infinity in the single-frequency case. In the dual-frequency case, the MDB's are somewhat smaller and they also increase less rapidly as the number of satellites decreases.

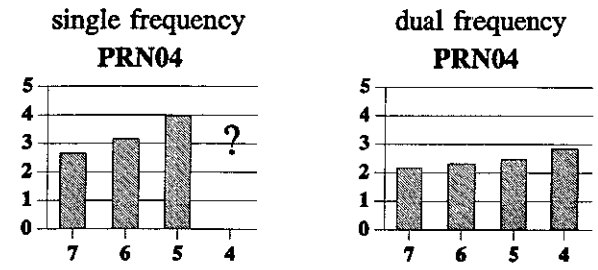

Figure 3: Ambiguity-float code-MDB's (m) of PRN 04 versus number of satellites; single frequency case (left) and dual-frequency case (right).

Figure 4 shows the case when the ambiguities are assumed known. In this case there is practically no difference between the single-fequency case and the dual-frequency case. This is due to the very high precision of the phase observables as compared to the precision of the code observables. In fact, when the ambiguity-fixed phase observables would be known exactly, the corre-

sponding baseline would be known exactly and the L_1 and L_2 single differenced code observables would then only have their clock errors as unknown parameters. The results of figure 4 follow therefore to a good approximation the simple rule

$$\mathrm{MDB} = \sigma_p \sqrt{\frac{2m\lambda_0}{m-1}} \tag{5}$$

where m denotes the number of satellites.

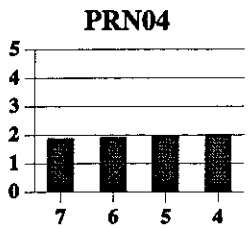

Figure 4: Ambiguity-fixed code-MDB's (m) of PRN 04 versus number of satellites.

Figure 5 shows the ambiguity-float phase-MDB's, expressed in L_1 phase cycles. They are shown for the case only 2 epochs of data are used (gray) and for the case 31 epochs of data are used (white). In the single-frequency case all but one of the MDB's are at the level of a few tenths of cycle. However when only four satellites are tracked, the MDB's blow up to an unacceptable level of over ten cycles. This does not happen in the dual-frequency case. In that case all MDB's stay at the level of a few tenths of a cycle.

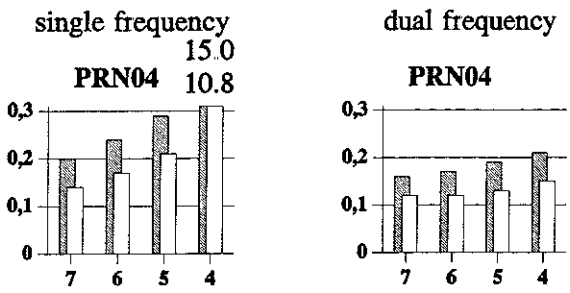

Figure 5: Ambiguity-float phase-MDB's (cycle) of PRN 04 versus number of satellites; single frequency case (left) and dual-frequency case (right).

Figure 6 shows the ambiguity-fixed phase-MDB's. Again only one epoch of data was used. A comparison between this figure and the previous one shows that the ambiguity-fixed MDB's using only a single epoch of data come close to the ambiguity-float MDB's based on the 31 epochs of data. And indeed one can show that these two type of MDB's are related through the scaling factor

$$\sqrt{1-\frac{1}{k}}$$

where k denotes the number of epochs used.

The above results are based on the assumption that $\sigma_p = 0.3$ m and $\sigma_\phi = 0.003$ m. It can be shown however that the precision of phase has (practically) no influence on the code-MDB's and that the precision of code has (practically) no influence on the phase- MDB's. This implies that the above results can easily be modified when different values for the standard deviations are used. For instance when the standard deviation of code is changed from 0.3 m to 0.1 m, the corresponding code-MDB's need to be divided by a factor of 3 as well. The same holds true for the phase-MDB's when changing the precision of phase.

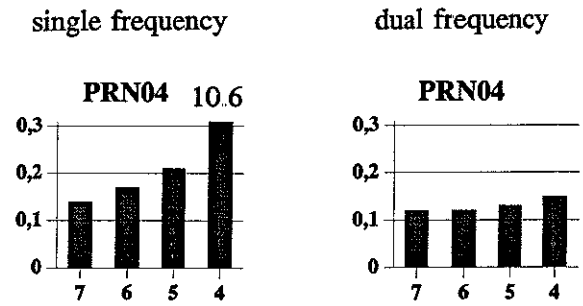

Figure 6: Ambiguity-fixed phase-MDB's (cycle) of PRN 04 versus number of satellites; single frequency case (left) and dual-frequency case (right).

4 AMBIGUITY RESOLUTION

GPS ambiguity resolution is the process of resolving the unknown cycle ambiguities of the double difference carrier phase data as *integers*. It is the key to high precision relative GPS positioning, when only short observation time spans are used. In this section we will investigate the system's ability to resolve the integer ambiguities when using the kinematic mode of operation. Ambiguity resolution is composed of two parts, the estimation part and the validation part.

4.1 ESTIMATION

When solving the system of observation equations (1), without the integer constraints included, one obtains the so-called *float* solution for the ambiguities. When using k epochs of data we thus have available the real-valued least-squares ambiguity vector $\hat{a}(k)$ and its variance matrix $Q_{\hat{a}(k)}$. This result is then used as input for the *integer* estimation step. It amounts to solving the integer

least-squares problem

$$\min_{a \text{ integer}} [\hat{a}(k) - a]^T Q^{-1}_{\hat{a}(k)} [\hat{a}(k) - a] \qquad (6)$$

Due to the integer constraint this problem cannot be solved by means of standard least-squares algorithms. Instead a search is needed for computing the integer minimizer $\check{a}$. With (near) real-time applications in mind it is of course of importance to keep the cycle- time needed to perform the necessary computations, at a minimum. The method of the Least-squares AMBiguity Decorrelation Adjustment (LAMBDA) has been developed to meet this requirement [16]. The steps involved in this method can briefly be described as follows (for more details, the reader is referred to [17, 18]). The global search space of integers is first replaced by a local one, the so-called ambiguity search space. It is defined as [19]

$$[\hat{a}(k) - a]^T Q^{-1}_{\hat{a}(k)} [\hat{a}(k) - a] \leq \chi^2 \qquad (7)$$

It is a multivariate ellipsoidal region, which is centred at $\hat{a}(k)$. Its shape is governed by the ambiguity variance matrix and its size can be controlled by choosing an appropriate value for the positive constant χ^2, see [20]. A two dimensional example of the search space is shown in figure 7.

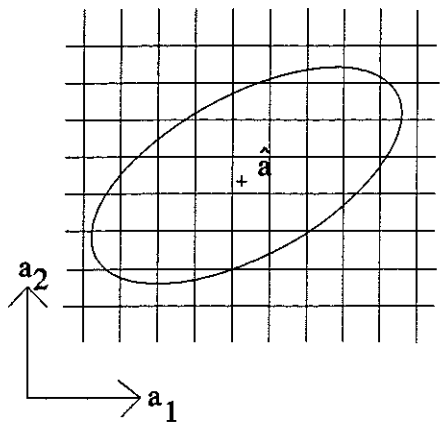

Figure 7: Two dimensional example of DD search space

Although the search for the integer least-squares ambiguities can in principle be based on the DD ambiguity search space (7), this is usually not an efficient approach because of the high correlation between the DD ambiguities, see [7]. The LAMBDA method therefore first transforms the DD ambiguities by means of a decorrelating ambiguity transformation $z = Z^T a$. As a result one obtains an equivalent, but transformed search space

$$[\hat{z}(k) - z]^T Q^{-1}_{\hat{z}(k)} [\hat{z}(k) - z] \leq \chi^2 \qquad (8)$$

In contrast to the original DD ambiguities, the transformed ambiguities have the property that they are largely decorrelated and of a high precision. Also the original DD search space has been moulded into a more spherical search space. A two dimensional example of the decorrelation process is shown in figure 8.

Due to the properties of the transformed ambiguities, the search for the integer least-squares ambiguities can now be performed in a very efficient manner. The search is based on scalar bounds which follow from applying a sequential conditional least-squares adjustment. How the actual search is executed is described in [18]. As a result of the search one obtains the integer least-squares solution $\check{z}$, which if needed, can be back-transformed to the integer least-squares solution of the original DD ambiguities, $\check{a} = Z^{-T}\check{z}$.

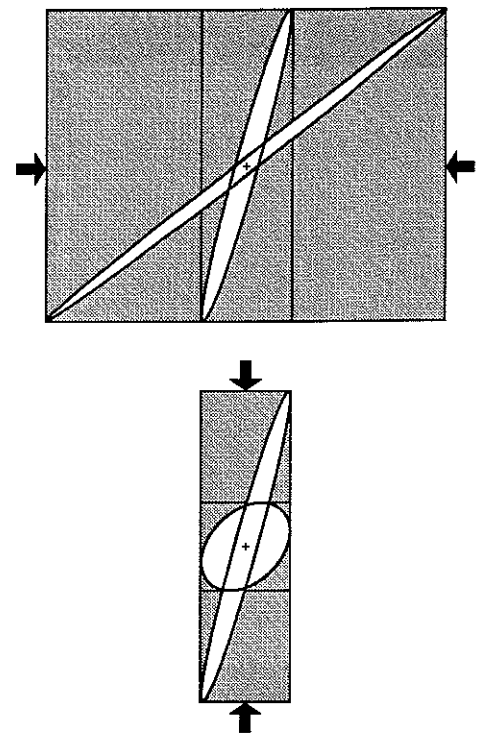

Figure 8: Two dimensional example of search space transformation through ambiguity decorrelation

4.2 VALIDATION

Estimation of the integer ambiguities is one thing, their validation however is quite another. One can always compute the integer least- squares ambiguities, whether the data are of poor quality or not, or whether the model used is adequate or not. The importance of validation is therefore to reduce the risk of accepting nonacceptable integer values for the ambiguities. In case of GPS this requires great care since a bias of a single cycle in the computed integer least-squares solution already can result in an unacceptable large baseline bias.

Ambiguity dilution of precision

It will be intuitively clear that the risk of computing an incorrect integer ambiguity solution must be related to the precision with which the real- valued least-squares ambiguities can be computed. Hence, if both the functional and stochastic model were specified correctly, the ambiguity variance matrix $Q_{\hat{a}(k)}$ must in some way contain information on one's expectation of being able to compute the correct integer ambiguities. The risk of having computed a wrong integer solution increases the poorer the ambiguity precision becomes.

To come up with a useful scalar measure for the ambiguity precision is not trivial. First, we are not dealing with a single ambiguity, but with a vector of ambiguities. They are correlated and their individual variances will generally differ. Secondly, we also have to take the arbitrariness into account by which the ambiguities are defined. Already in case of the DD ambiguities, different sets of DD ambiguities can be recognized when different satellites are chosen as the reference satellite. Thus in order to truely measure the intrinsic precision characteristics of the ambiguities, one should have a measure that is invariant for the arbitrary choice one has in defining integer ambiguities. Such an ambiguity dilution of precision (ADOP) measure was introduced in [6] as

$$\text{ADOP} = \sqrt{\det Q_{\hat{a}(k)}}^{\frac{1}{n}} \quad \text{(cycle)} \tag{9}$$

where n is the order of the ambiguity variance matrix. It can be shown that the ADOP is indeed invariant for the whole class of admissible ambiguity transformation. It can also be shown that it equals the geometric mean of the sequential conditional standard deviations of the ambiguities. Thus in case of the decorrelated ambiguities obtained with the LAMBDA method, it approximates the geometric mean of the unconditional standard deviations of the transformed ambiguities. Ambiguity resolution can therefore expected to be successful when the ADOP is at the few tenths of a cycle level or smaller.

Figure 9 shows some typical values that can be achieved in case of single-epoch based ambiguity resolution ($k = 1$). In this case (single or dual frequency) code data are needed per se to be able to compute a float solution. Shown are, for both the single and dual frequency case (phase and code), the standard deviation of one of the DD ambiguities and the ADOP, both as function of the number of satellites used. The ambiguity standard deviation gets of course poorer as the number of satellites decreases and improves by a factor of $\sqrt{2}$ when one switches from the single-frequency case to the dual-frequency case. In all cases the standard deviations are far larger than the one cycle level. But as it was pointed out above, no inference can be made from these individual ambiguity standard deviations, since they do not take the presence of correlation into account and because they are dependent on the arbitrary ambiguity definition as well. This is not the case with the ADOP. As the figure shows for the ADOP's, there is a significant improvement in the single-frequency case when the number of satellites increases. Likewise there is a significant improvement when switching from the single-frequency case to the dual- frequency case, in particular when the satellite redundancy is small. Based on these results one would expect instantaneous ambiguity resolution to be feasible in the dual-frequency case, but problematic or even impossible in the single-frequency case when the number of satellites drops below six.

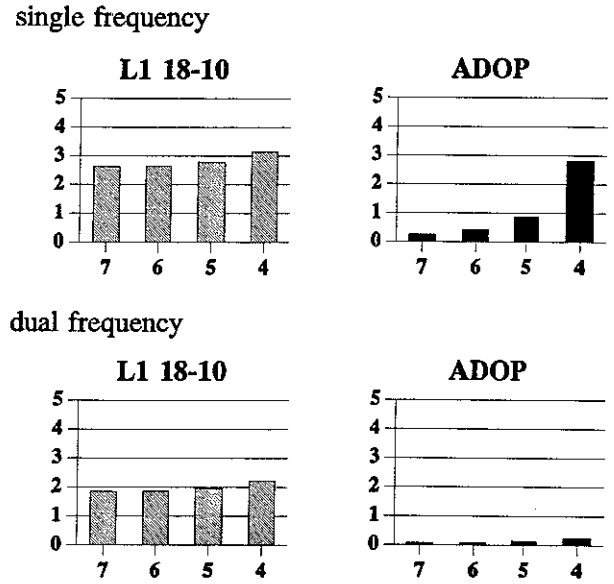

Figure 9: Ambiguity precision: ambiguity standard deviation of DD ambiguity 18-10 (cycle) versus number of satellites and ADOP (cycle) versus number of satellites; single frequency (top), dual-frequency (bottom), ambiguity standard deviation (left), ADOP (right)

Testing the integer least-squares solution

The real test for answering the question whether or not the computed integer least-squares solution can be accepted, should of course be based on actual data. It is customary to make a distinction between two type of tests, the acceptance test and the discrimination test. Here we will follow [21]. The acceptance and discrimination test respectively, read

$$\frac{\breve{\sigma}^2}{\hat{\sigma}^2} \leq (C_1)^2 \tag{10}$$

and

$$\frac{\breve{\sigma}'^2}{\breve{\sigma}^2} \geq (C_2)^2 \tag{11}$$

where $\hat{\sigma}^2$ and $\check{\sigma}^2$ are the estimated variance factors of unit weight based on, respectively, the float and fixed solution, and where $\check{\sigma}'^2$ is the corresponding value based on $\check{a}'$, the second most-likely integer ambiguity solution. The second most-likely integer ambiguity vector produces the last but one smallest value of the objective function of (6). The 'critical values' were chosen as $C_1 = 5.0$ and $C_2 = 1.2$

Although the discrimination test (11) is formulated in the DD ambiguities, it can be formulated in the transformed ambiguities of the LAMBDA method as well. The test statistic is, as it should be, invariant for this transformation

The first test infers the likelihood of the most-likely integer solution. The most-likely solution is of course by definition the integer least- squares solution. The second test infers whether the second most-likely integer solution differs sufficiently in likelihood from the most-likely solution. If both tests are passed successfully, the decision is made to accept the integer least-squares solution as being correct. It is remarked that although the above two tests seem to work satisfactorily in practice, a theoretical basis of these tests (e.g. knowledge of probability density function) is still lacking.

In the following we will concentrate on the second test for cases for which the first test was passed successfully. From the full session of the nonstationary baseline 15-39 (the van is driven from about 2 km to over 12 km from the reference and back again), all 2421 epochs of dual-frequency data were first used to compute the overall integer least-squares solution of the ambiguities. This solution provided our 'ground truth', which we believe to be acceptable due to the cleaness of the data and the length of the observation time span. Then the full session was partitioned in 40 batches of half a minute, each spaced by again a half minute. This gave us 40 experiments to test for ambiguity resolution in a kinematic mode

Based on previous experience [11], instantaneous ambiguity resolution using seven satellites most often results in a successful fixing of the ambiguities. Having figure 9 in mind, we therefore concentrated our computations on the use of only five satellites (PRN's 04, 10, 16, 27 and 18). For the dual-frequency case it was found that all single-epoch integer solutions were in agreement with the 'ground truth'. However, not all of these 40 solutions passed the above discrimination test successfully. Four single-epoch solutions were rejected by this test. In these four cases, additional epochs were needed to pass the test. The number of additional epochs needed varied from only a few to more than thirty

The conclusion from these 40 experiments using five satellites is thus that dual-frequency instantaneous ambiguity resolution seems possible at a high success rate. For the single-frequency case however a completely different result was obtained. In 7 percent of the 40 experiments the discrimination test was not even passed successfully after using all of the 31 epochs available per experiment. In 55 percent of the cases the discrimination test was declared accepted, although the corresponding integer solution failed to agree with the 'ground truth'. Thus only in 38 percent of the cases did the integer solution, that passed the discrimination test, agree with the 'ground truth'. And only four of them were obtained instantaneously. The conclusion is thus clearly that single-frequency ambiguity resolution, based on only five satellites, poses serious problems. A snapshot listing of the single-frequency analysis is given in table 1.

exp.	accepted by test	at epoch	correct?
13	Y	1	Y
14	Y	2	Y
15	Y	1	N
16	Y	1	N
17	Y	13	Y
18	Y	1	N
19	Y	1	N
20	Y	1	N
21	?	> 31	
22	Y	8	N
23	Y	1	N
24	Y	30	N

Table 1: Ambiguity resolution: single frequency phase and code using five satellites

5 KINEMATIC POSITIONING

In this section we will describe the kinematic positioning performance of the experiment. First however we consider the effect of antenna rotation on the phase observations.

5.1 CARRIER PHASE WRAP-UP

Carrier phase wrap-up will occur when the antenna's are rotated while tracking the GPS signals [22-24]. This will thus also happen when using the kinematic mode of operation. To get some insight into the effects involved a small test was conducted. Two simultaneously tracking antenna's were used, of which one was at rest while the other was rotating. The L_1 minus L_2 phase combination $(\phi_1 - \phi_2)$, expressed in meters, for a single satellite is shown in figure 10 for both antenna's.

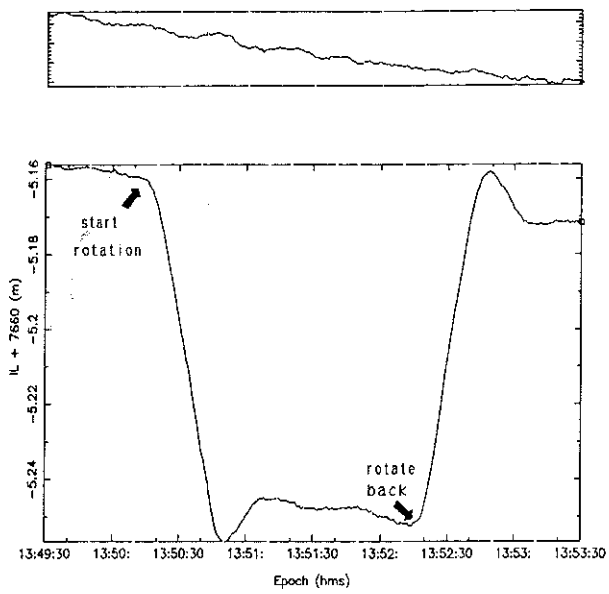

Figure 10: Ionosphere combination for antenna at rest (top) and for a rotating antenna (bottom).

The values shown were multiplied with the factor 1.546 so as to obtain a (relative) estimate of the ionospheric delay as it would be found for the L_1 code observable. Note that the scale of the vertical axis of the top-figure equals that of the bottom-figure. The horizontal axis spans 4 minutes. In the $1.546(\phi_1 - \phi_2)$ combination all common effects, like the geometric range, the clock error and the tropospheric range, are eliminated. The only remaining effects are, respectively, the ionospheric delay, the phase- ambiguities and the instrumental delays. Thus in case of a nonrotating antenna this combination will show primarily the time behaviour of the ionosphere. In case of figure 10 (top) this effect is about 2 cm over 4 minutes. However when the antenna is rotated in about 30 seconds over a full 360 degrees, the 'wrap-up' effect shows up and amounts to $1.546 \times 0.054 = 0.083$ m. The value 0.054 is the difference between the L_2 and the L_1 wavelength. The effect is thus about 8 cm, see figure 10 (bottom). This effect gets eliminated again when the antenna is rotated back over the same angle (note: the figure shows some overshooting, which is believed to be due to internal filtering of the receiver).

The 'wrap-up' shown in the figure, by rotating the antenna around the bore-sight axis, was found to be the same on all channels. This has the fortunate consequence that while adjusting for the kinematic model, the effect gets lumped with the unknown clock error. Hence the effect gets eliminated when working with DD observables, just like the double differencing gets rid of the clock error. The kinematic positioning results are therefore not affected by the above 'wrap-up'.

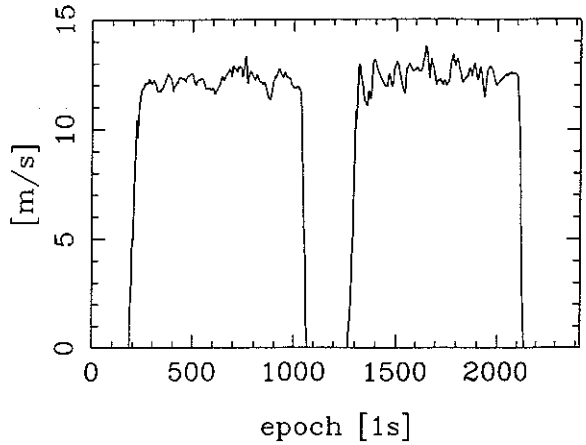

Figure 11: Velocity profile (m/s) of van.

5.2 BASELINE REPEATIBILITY

For the baseline repeatibility, we first considered the baseline 15 (stationary reference) to 39 (rover on van). The van started at about 2 km from the reference and made a two-way trip with the turning point at about a 12 km distance. The velocity profile of the van during the two- way trip is shown in figure 11. It was computed from the displacement in three dimensions over one second intervals. There are three static periods, one at the beginning, one at the end and one halfway just before the turn was made. The van drove at slightly over 40 km/hr.

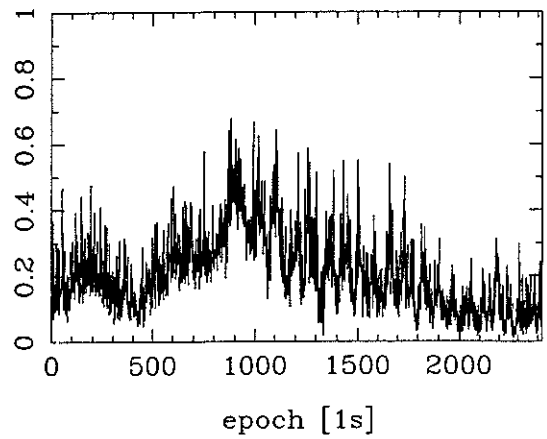

Figure 12: LOM test-statistic $T(i)$ divided by its critical value.

Single-frequency phase and code data (2421 epochs, one second sampling rate) of 7 satellites were used to compute the van's trajectory. The ambiguities could be

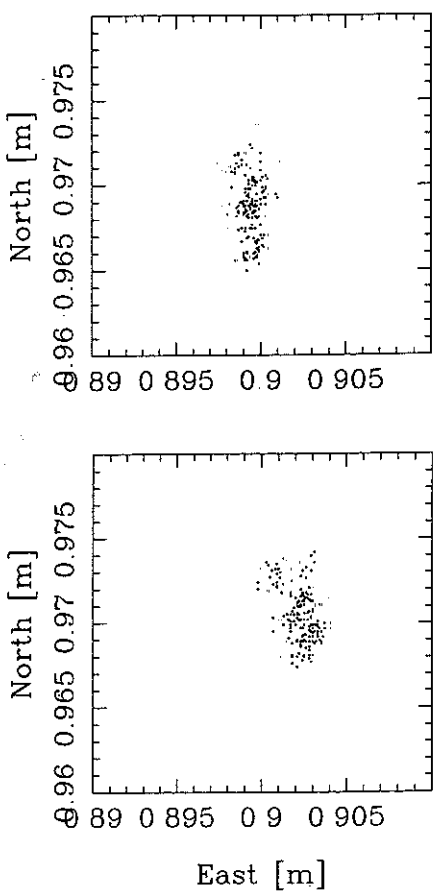

Figure 13: Scatter plots: first static period of baseline 15-39 (top) and of baseline 28-39 (bottom)

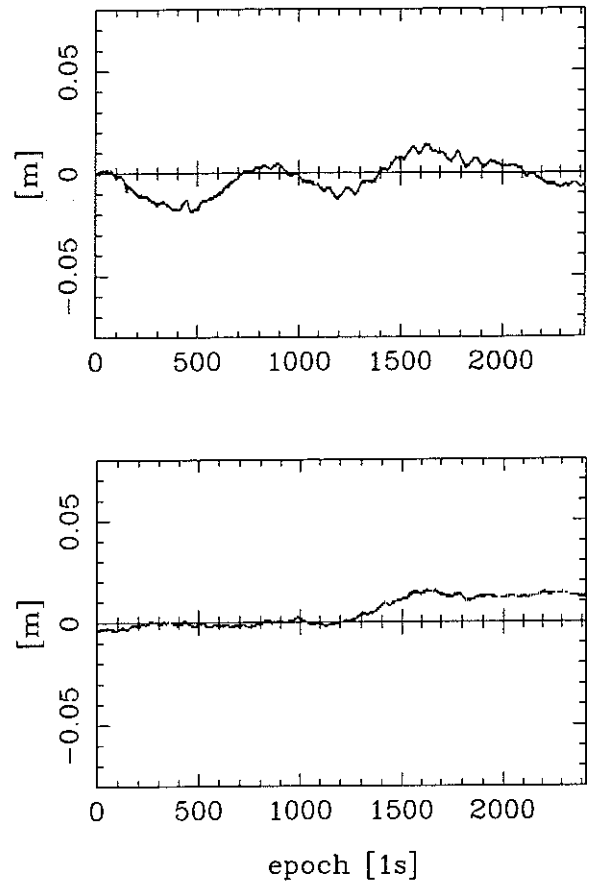

Figure 14: Kinematic solution of stationary baseline 15-28 in North (top) and East (bottom)

fixed right away at the very first epoch. The results that will be shown are therefore based on using single-frequency ambiguity-fixed phase and code data. The code data is thus included, but it will be clear that their contribution will be very marginal due to the relatively poor precision of code.

The samples of the LOM test-statistic $T(i)$ divided by its critical value are shown in figure 12 as function of time. The values shown all stay well below the value of 1. In the model validation no outliers in the code data nor cycle slips in the phase data were encountered. The fact that the mean of the test-statistic is significantly smaller than its expectation may indicate that a too pessimistic stochastic model was used. A dependence of the noise of the observables on the receiver dynamics does not show up in the graph, nor does it show a relation with the baseline length. The results do make us suspect the presence of some systematic time behaviour.

To get an impression of the empirical precision of positioning, the three static periods were considered. Since all three static periods showed the same behaviour, only the first scatter plot is shown in figure 13 (top). These results show that the short-term repeatibility of the kinematic positioning is excellent (spread at the level 0.5-1 cm). However, these results will not show the presence of any bias. We therefore repeated the same computations but now with the use of the data of the stationary receiver at point 28. Since the baseline coordinates of the stationary baseline 15-28 were known (independently determined from long time span data), the scatter plot of the kinematic baseline 28-39 can also be referenced with respect to point 15. The results are shown in figure 13 (bottom). Comparison of the two scatter plots shows indeed the presence of some small bias (at the 1 cm level). The same small level was found for the two other static periods.

Although the bias is sufficiently small for most surveying applications, its presence indicates that our simple model is not capable yet of catching all systematic effects. This is also apparant if one considers the kinematic solution of the stationary basline 15-28. Figure 14 shows the kinematic solution referenced with respect to the reference coordinates of the baseline. Although the size of the bias is sufficiently small to be acceptable, there is still clearly a systematic time behaviour present in the positioning results (e.g. short and long periodic). Our analysis of the tropospheric delays, the ionospheric delays and of multipath did not indicate a clear culprit.

although multipath was clearly present in the data from satellite PRN 27. More analysis is therefore needed to be able to trace the origin of the above systematic but small time behaviour.

6 ACKNOWLEDGEMENTS

The first author's contribution was done under contract with the Survey Department of the Rijkswaterstaat. Dennis Odijk and Niels Jonkman assisted in running the experiment. Two of the three receivers were kindly provided by the Triangulation Department of the Dutch Cadastre

7 REFERENCES

[1] Hofmann-Wellenhof, B., H. Lichtenegger, J. Collins (1994): *Global Positioning System: Theory and Practice* 3rd edition. Springer Verlag

[2] Leick, A. (1995): *GPS Satellite Surveying* 2nd edition, John Wiley, New York.

[3] Borre, K. (1995): *GPS i landmaelingen*, Aalborg.

[4] Kleusberg, A., P.J.G. Teunissen (Eds.) (1996): *GPS for Geodesy*, Lecture Notes in Earth Sciences, Vol. 60, Springer Verlag.

[5] Goad, C.C. (1996): Short distance GPS models (Ch. 7). In: *GPS for Geodesy* Lecture Notes in Earth Sciences, Vol. 60. Springer Verlag.

[6] Teunissen, P.J.G. (1997): A canonical theory for short GPS baselines *Journal of Geodesy*, in print.

[7] Teunissen, P.J.G., P.J. de Jonge, C.C.J.M. Tiberius (1997): The least-squares ambiguity decorrelation adjustment: its performance on short GPS baselines and short observation time spans *Journal of Geodesy*, in print

[8] Remondi, B.W. (1986): Performing cm-level surveys in seconds with GPS carrier phase: initial results. *Journal of Navigation*, Vol. III, The Institute of Navigation.

[9] Frei, E. (1991): *Rapid differential positioning with the Global Positioning System*. In: Geodetic and Geophysical Studies in Switzerland, Vol. 44.

[10] Hwang, P.Y.C. (1991): Kinematic GPS for differential positioning: resolving integer ambiguities on the fly. In: *Navigation*, Vol. 38, No. 1, pp. 1-15

[11] Tiberius, C.C.J.M., P.J. de Jonge (1995): Fast positioning using the LAMBDA method. In: *Proc DSNS-95*, Bergen, Norway, April 24-28, 1995, Paper No. 30.

[12] Lan, H., M.E. Cannon (1996): Development of a real-time kinematic GPS system: system design, performance and results. In: *Proc. ION technical Meeting*, Santa Monica, CA, Jan. 22-24, 1996, pp 605-613.

[13] Teunissen, P.J.G. (1997): Quality control and GPS In: Lecture Notes 2^{nd} International School *GPS for Geodesy*, Chapter 7, Delft, The Netherlands, March 2-8, 1997

[14] Teunissen, P.J.G., M.A. Salzmann (1989): A recursive slippage test for use in state-space filtering. *Manuscripta Geodaetica*, Vol. 14, No. 6, pp. 383-390.

[15] Teunissen, P.J.G. (1990): An integrity and quality control procedure for use in multi sensor integration. In: *Proc. ION GPS-90*, Colorado, USA, Sept. 19-21, pp. 513-522

[16] Teunissen, P.J.G. (1993): Least-squares estimation of the integer GPS ambiguities. Invited Lecture, Section IV Theory and Methodology, IAG General Meeting, Beijing, China, August 1993. Also in: *LGR Series*, No. 6, Delft Geodetic Computing Centre.

[17] Teunissen, P.J.G. (1995): The least-squares ambiguity decorrelation adjustment: a method for fast GPS integer ambiguity estimation. *Journal of Geodesy*, Vol. 70, No. 1-2, pp. 65-82.

[18] Jonge de, P.J., C.C.J.M. Tiberius (1996): The LAMBDA method for integer ambiguity estimation: implementation aspects. *LGR Series*, No. 12, Delft Geodetic Computing Centre. Also available through the Internet: http://www.geo.tudelft.nl/mgp/

[19] Teunissen, P.J.G., C.C.J.M. Tiberius (1994): Integer least-squares estimation of the GPS phase ambiguities. In: *Proc. KIS94*, Banff, Canada, Aug. 30-Sept. 2, pp. 221-231.

[20] Teunissen, P.J.G., P.J. de Jonge, C.C.J.M. Tiberius (1996): The volume of the GPS ambiguity search space and its relevance for integer ambiguity resolution. In: *Proc. ION GPS-96*. Kansas City, USA, Sept. 17-20, pp. 889-898

[21] Rothacher, M., L. Mervart (Eds.) (1996): Bernese GPS software version 4.0. Astronomical Institute, University of Berne, September 1996.

[22] Wu, J. T., S. C. Wu, G. A. Hajj, W. I. Bertiger, S. M. Lichten (1993): Effect of antenna orientation on GPS carrier phase. *Manuscripta Geodaetica*, Vol. 18, pp. 91-98.

[23] Tetewsky, A., F. Mullen (1997): Carrier phase wrap-up induced by rotating GPS antennas. *GPS World*, February 1997, pp. 51-57.

[24] Storm van Leeuwen (1997): Personal communication, National Aerospace Laboratory NLR.